International Journal of Chemical, Materials and Biomolecular Sciences
ISSN: 2415-6620
Vol:4, No:8, 2010

Mathematical Simulation of Bubble Column Slurry Reactor for Direct Dimethyl Ether Synthesis Process from Syngas

Zhen Chen, Haitao Zhang, Weiyong Ying, Dingye Fang

***Abstract*—**Based on a global kinetics of direct dimethyl ether **(**DME) synthesis process from syngas, a steady-state one-dimensional mathematical model for the bubble column slurry reactor (BCSR) has been established. It was built on the assumption of plug flow of gas phase, sedimentation-dispersion model of catalyst grains and isothermal chamber regardless of reaction heats and rates for the design of an industrial scale bubble column slurry reactor. The simulation results indicate that higher pressure and lower temperature were favorable to the increase of CO conversion, DME selectivity, products yield and the height of slurry bed, which has a coincidence with the characteristic of DME synthesis reaction system, and that the height of slurry bed is lessen with the increasing of operation temperature in the range of 220-260℃. CO conversion, the optimal operation conditions in BCSR were proposed.

***Keywords*—**alcohol/ether fuel, bubble column slurry reactor, global kinetics, mathematical model

I. Introduction

CHINA is a country with rich coal, lacking oil and poor gas and forty percent of crude oil must be imported with the development of world economy, it is urgent that how to highly efficient utilization our coal resource. In recent year, there are hot spots to develop new chemical energy technologies in coal industry, such as syngas transformation to methanol/dimethyl ether process. Dimethyl ether is an important chemical and intermediate for the production of gasoline, ethylene, aromatics and other chemicals, and it has an increasing application as ultra-clean fuel for diesel engines and as ozone friendly propellant for aerosol industry.

Direct DME synthesis process is in traditional tubular fixed-bed reactor, in which the syngas mostly reacted on surface of the solid catalysts. The advantage of this method is high CO conversion and high selectivity for DME. But for methanol/ dimethyl ether synthesis is a strongly exothermal reaction, it will cause run-away which can detract seriously from the selectivity of catalysts and the catalyst irreversibly deactivated. So DME direct synthesis has received growing attention in a bubble slurry reactor [1] for its dramatic economic value and theoretical significance for the alleviation of the thermodynamics equilibrium limitation of methanol synthesis. The syngas bubbles are diffused to surface of the catalysts through inert medium oil that has high specific thermal capacity, and then reacted to DME in the three-phase slurry reactor. Due to effective heat transfer, the whole reaction bed can be regard as an isothermal chamber. But the deactivation problem of catalysts must be considered for the existence of water [2] adhering to the surface of catalysts. If the catalyst is sufficiently active, the capacity of the reactor will be limited by the rate of diffusion to or from the catalyst surface.

There are normally two types of the catalysts for single-step process: bi-functional hybrid catalysts [3]-[4] which are commonly the mechanical mixture of methanol synthesis catalyst ($CuO\text{-}ZnO\text{-}Al_2O_3$) and methanol dehydration catalyst (γ-Al_2O_3/ZSM-5) and liquid slurry catalysts [5] which are prepared by a novel complete liquid-phase technology and have small and uniform granularity, high dispersion degree, lower viscosity and higher activity stability. And these slurry catalysts also contain two types of active sites respectively. The research of DME direct synthesis process is mainly focused on discrimination of bi-functional catalysts, development of different kinetic models and relevant reactor design of mathematical simulation either in a fixed-bed reactor [6] or fluidized bed reactor [7]. Nie *et al* [8] has been presented an intrinsic kinetics and reactor simulation model for DME direct synthesis from syngas over a bi-functional catalyst of $CuO\text{-}ZnO\text{-}Al_2O_3$ and γ-Al_2O_3 in a fixed-bed reactor.

In this paper, by fitting our experimental data, a global kinetic model for liquid phase DME direct synthesis has been proposed subsequently over Cu-Zn-Al-Zr slurry catalyst based

Financial support by a grant from the Major State Basic Research Development Program of China (973 Program) (No. 2005CB221205).

Zhen Chen was with Department of Light Chemistry and Environment Engineering, Shandong Institute of Light Industry, Ji'nan Shandong 250353 China. He is now with Engineering Research Center of Large Scale Reactor Engineering and Technology, Ministry of Education, State Key Laboratory of Chemical Engineering, East China University of Science and Technology, Shanghai 200237 China (e-mail: chenzhensd@hotmail.com).

Haitao Zhang is with Engineering Research Center of Large Scale Reactor Engineering and Technology, Ministry of Education, State Key Laboratory of Chemical Engineering, East China University of Science and Technology, Shanghai 200237 China (e-mail: zht@ecust.edu.com).

Weiyong Ying is with Engineering Research Center of Large Scale Reactor Engineering and Technology, Ministry of Education, State Key Laboratory of Chemical Engineering, East China University of Science and Technology, Shanghai 200237 China (phone: 86-21-64252193; fax: 86-21-64252192; e-mail: wying@ecust.edu.com).

Dingye Fang is with Engineering Research Center of Large Scale Reactor Engineering and Technology, Ministry of Education, State Key Laboratory of Chemical Engineering, East China University of Science and Technology, Shanghai 200237 China (e-mail: dyfang@ecust.edu.com).

on Langmuir-Hinshelwood mechanism. And it has been further developed a steady state one-dimensional mathematical model in an industrial scale BCSR based on reasonable assumption and simplifications for the design of the reactor. A few literatures[9] have been published for the kinetics and mathematical model in BCSR for direct DME synthesis from syngas over Cu-Zn-Al-Zr slurry catalyst.

II. Development of Reactor Model in BCSR

A. Reaction Kinetic Scheme

The main catalytic reactions in direct DME synthesis process are considered as follows:

methanol synthesis from CO hydrogenation:

$$CO + 2H_2 \rightleftharpoons CH_3OH \quad (1)$$

methanol synthesis from CO_2 hydrogenation:

$$CO_2 + 3H_2 \rightleftharpoons CH_3OH + H_2O \quad (2)$$

methanol dehydration to DME:

$$2CH_3OH \rightleftharpoons CH_3OCH_3 + H_2O \quad (3)$$

water gas shift reaction (WGS):

$$CO + H_2O \rightleftharpoons CO_2 + H_2 \quad (4)$$

direct synthesis of DME from CO hydrogenation:

$$2CO + 4H_2 \rightleftharpoons CH_3OCH_3 + H_2O \quad (5)$$

and direct synthesis of DME from CO_2 hydrogenation:

$$2CO_2 + 6H_2 \rightleftharpoons CH_3OCH_3 + H_2O \quad (6)$$

According to the phase law, the number of independent reactions in the dimethyl ether synthesis process from syngas is three. So the reaction schemes of DME direct synthesis can be explained by the combination of methanol synthesis from CO hydrogenation and from CO_2 hydrogenation and methanol dehydration to DME, i.e. (1)-(3).

B. Global Kinetics of DME Synthesis

By choosing CO, CO_2 and DME as key components and chemical equation (1), (2), and (3) as reaction system, the global kinetics equations for methanol synthesis from CO, CO_2 and methanol dehydration to DME based on Langmiur-Hinshelwood mechanism were expressed as follows

$$r_{CO} = \frac{-dN_{CO}}{dW} = \frac{k_1 f_{CO} f_{H_2}^2 (1-\beta_1)}{(1 + K_{CO} f_{CO} + K_{CO_2} f_{CO_2} + K_{H_2} f_{H_2})^3} \quad (7)$$

$$r_{CO_2} = \frac{-dN_{CO_2}}{dW} = \frac{k_2 f_{CO_2} f_{H_2}^3 (1-\beta_2)}{(1 + K_{CO} f_{CO} + K_{CO_2} f_{CO_2} + K_{H_2} f_{H_2})^4} \quad (8)$$

$$r_{DME} = \frac{dN_{DME}}{dW} = \frac{k_3 f_M (1-\beta_3)}{(1 + \sqrt{K_M f_M})^2} \quad (9)$$

where $\beta_1 = \frac{f_M}{K_{f1} f_{CO} f_{H_2}^2}$, $\beta_2 = \frac{f_M f_{H_2O}}{K_{f_2} f_{CO_2} f_{H_2}^3}$, $\beta_3 = \frac{f_{DME} f_{H_2O}}{K_{f_3} f_M^2}$, β_i refers to the equilibrium degree of the ith independent reaction, respectively, and f_j stands for the fugacity of component j, which is calculated by the SHBWR equation of state[10]. K_{fi} is the equilibrium constant in form of each component fugacity for the ith independent reactions, and the thermodynamic calculation expressions were given by the following relations [11]

$$K_{f_1} = \exp[13.1652 + \frac{9203.26}{T} - 5.92839 \ln T - 0.352404 \times 10^{-2} T + 0.102264 \times 10^{-4} T^2 - 0.769446 \times 10^{-8} T^3 + 0.238583 \times 10^{11} T^4] \times (0.10135)^{-2} \quad (10)$$

$$K_{f_2} = \exp[1.6654 + \frac{4553.34}{T} - 2.72613 \ln T - 1.106294 \times 10^{-2} T + 0.172060 \times 10^{-4} T^2 - 1.106294 \times 10^{-8} T^3 + 0.319698 \times 10^{11} T^4] \times (0.101325)^{-2} \quad (11)$$

$$K_{f_3} = \exp[-9.3932 + \frac{3204.71}{T} + 0.83593 \ln T + 2.35267 \times 10^{-3} T - 1.8736 \times 10^{-6} T^2 + 5.1606 \times 10^{-10} T^3] \quad (12)$$

Reaction rate constant as model parameters, namely k_i, can be defined by Arrhenius relations:

$$k_i = k_{0i} \exp(-E_i / RT) \quad (i=1, 2, 3) \quad (16)$$

and the adsorption equilibrium constant, namely K_j, can be defined by Van't Hoff relations:

$$K_j = K_{0j} \exp(-E_j / RT) \quad (j=CO, CO_2, H_2, M) \quad (17)$$

where k_{0i} or K_{0j} is the pre-exponential factor, E_i is the apparent activation energy for the ith independent reaction , and E_j is the apparent adsorption heat for the adsorption equilibrium constant of component j.

According to the total of 25 experimental data shown in Table 1, the parameters values of global kinetic model in CSTR, with a 95% confidence internal, are listed in Table I.

TABLE I
Regression Parameters for the Global Kinetics Model

Parameters	Pre-exponential factors ($mol \cdot g^{-1} \cdot h^{-1}$)	Apparent activation energy ($J \cdot mol^{-1}$)
k_1	7.704×10^3	26348.74
k_2	8.558×10^2	20587.82
k_3	1.8455×10^2	25845.97
K_{CO}	5.76×10^{-6}	-33499.95
K_{CO2}	9.66×10^{-6}	-20830.80
K_{H2}	4.307×10^{-2}	-20692.27
K_M	2.888	-20171.23

C. Reactor Model Assumptions

Zhao [12] has discussed systematically bubble column slurry reactor and relevant descriptions in detail of hydromechanics, transport processes and mathematical model for commercial demonstration plants. The assumption of plug flow in gas phase is usually valid, but there are two flow patterns for slurry phase:

fully back-mixing and plug flow. Govindarao [13]-[14] demonstrated generalized mathematical model in BCSR on the hypothesis of axial diffusion in gas-liquid-solid phase, boundary heat transfer and grain sedimentation-dispersion model for methanol synthesis process.

The mathematical model in the BCSR model can be made further assumptions as follows:

1) Due to the liquid phase inert carrier with high thermal conductivity and heat capacity, Bubble column slurry reactor can be regarded as an isothermal chamber under high turbulence, in which heat transfer can be negligible.
2) The bubble phase is in plug flow, and gas back-mixing can be negligible.
3) The liquid phase is assumed to be fully back-mixing flow in high space velocity and high turbulence.
4) The components of syngas are sparingly soluble in a liquid paraffin inert carrier, and then mass transfer resistance of gas phase can be ignored.
5) Mass transfer resistance was ignored in the liquid-solid phase, and internal diffusion effectiveness factors of the catalyst are close to 1 because of adapting to ultrafine slurry catalyst.
6) Catalyst concentration distribution along the bed height obeys the grains sedimentation-dispersion model, which take into consideration the influence of both liquid phase axial back-mixing and grain sedimentation.
7) Liquid properties, such as gas holdup, mass transfer coefficient, and diffusion coefficient, are kept constant along the column bed.

D.Mathematical Model in BCSR

Having assumed uniform temperature in the column bed, we only have to consider material balance equation for component *j* in the gas-liquid-solid three phase, which are as follows:

The main effect factors of the gas phase concentration-time history are axial back-mixing of gas phase, superficial gas velocity and gas-liquid mass transfer. In the steady state conditions, the mass balance equation for the component *j* in gas phase is given by

Gas phase:

$$D_G\frac{d^2C_{G,j}}{dZ^2}-u_G\frac{dC_{G,j}}{dZ}-k_{L,j}a_L\left(C^*_{G,j}-C_{L,j}\right)=0 \tag{15}$$

The main effect factors of the liquid phase concentration-time history are axial back-mixing of liquid phase, superficial liquid velocity, gas-liquid mass transfer and liquid-solid mass transfer. In the steady state, the mass balance equation for the component *j* in liquid phase is given by

Liquid phase:

$$D_L\frac{d^2C_{L,j}}{dZ^2}-u_L\frac{dC_{L,j}}{dZ}+k_{L,j}a_L\left(C^*_{G,j}-C_{L,j}\right)-k_{S,j}a_SC_{cat}\left(C_{L,j}-C_{S,j}\right)=0 \tag{16}$$

The main effect factors of the solid phase concentration-time history are gas-liquid mass transfer and reaction rate of each catalytic reaction. In the steady state, the mass balance equation for the component *j* in solid phase is given by

Solid phase:

$$k_{S,j}a_SC_{cat}\left(C_{L,j}-C_{S,j}\right)-\sum_{i=1}^{3}C_{cat}\cdot\nu_{i,j}r_{i,j}=0 \tag{17}$$

Catalyst grains sedimentation-dispersion model can be expressed by

$$D_S\frac{d^2C_{cat}}{dZ^2}+u_p\frac{dC_{cat}}{dZ}=0 \tag{18}$$

Substituting (17) into (16), we can obtain:

$$D_L\frac{d^2C_{L,j}}{dZ^2}-u_L\frac{dC_{L,j}}{dZ}+k_{L,j}a_L\left(C^*_{G,j}-C_{L,j}\right)-\sum_{i=1}^{3}C_{cat}\cdot\nu_{i,j}r_{i,j}=0 \tag{19}$$

Further simplification can be made by assuming that the Herry's law applies to each gas-liquid phase component. Combining with the assumptions 2), (15) can be simplified to

$$u_G\frac{dC_{G,j}}{dZ}+k_{L,j}a_L\left(\frac{C_{G,j}}{m}-C_{L,j}\right)=0 \tag{20}$$

Comparing to the whole reaction bed, the liquid phase is non- flowing, then (19) is simplified to

$$D_L\frac{d^2C_{L,j}}{dZ^2}+k_{L,j}a_L\left(\frac{C_{G,j}}{m}-C_{L,j}\right)-\sum_{i=1}^{3}C_{cat}\cdot\nu_{i,j}r_{i,j}=0 \tag{21}$$

This mathematical model is based on the global kinetics model for the catalytic reaction in continuous stirred tank reactor, which take into account the complicated physical process such as mass transfer and diffusion in the gas-liquid-solid three phase. Then (21) can be further simplified to

$$k_{L,j}a_L\frac{C_{G,j}}{m}=\sum_{i=1}^{3}C_{cat}\cdot\nu_{i,j}r_{i,j} \tag{22}$$

Substituting Eq. (22) into Eq. (20), we can obtain:

$$u_G\frac{dC_{G,j}}{dZ}+\sum_{i=1}^{3}C_{cat}\cdot\nu_{i,j}r_{i,j}=0 \tag{23}$$

For the grains sedimentation-dispersion model (18), Smith [15] provided the simplified calculation equations which is shown as the following

$$C_{cat}=C^0_{cat}\exp(Gx) \tag{24}$$

Combining (23) with (24), the one-dimensional mathematical model for the three-phase bubble column slurry reactor has been established, which was considered to be the influence of catalyst grain sedimentation on reaction process and macro dynamics process.

For the complicated reaction process of alcohol/ether fuel direct synthesis from syngas, we chose methanol synthesis from CO hydrogenation and CO_2 hydrogenation and methanol dehydration as the independent reactions, and chose CO, CO_2, and DME as key components. The total transient flux of the gas phase in the column can be calculated from the overall material balance.

$$\frac{N_{T,in}}{N_T}=\frac{1-2y_{CO}-2y_{CO_2}}{1-2y_{CO,in}-2y_{CO_2,in}} \tag{25}$$

Hence, the transient flux of each key component can be expressed by

$$N_j=N_{T,in}\cdot\frac{1-2y_{CO,in}-2y_{CO_2,in}}{1-2y_{CO}-2y_{CO_2}}\cdot y_j \quad (j=\text{CO, CO2, DME}) \tag{26}$$

Differential equations of (26) are given by

$$\begin{cases} dN_{CO} = B\left[(1-2y_{CO_2})dy_{CO} + 2y_{CO}dy_{CO_2}\right] \\ dN_{CO_2} = B\left[(1-2y_{CO})dy_{CO_2} + 2y_{CO_2}dy_{CO}\right] \\ dN_{DME} = B\left[(1-2y_{CO}-2y_{CO_2})dy_{DME} + 2y_{DME}(dy_{CO}+dy_{CO_2})\right] \end{cases} \quad (27)$$

where

$$B = N_{T,in} \cdot \frac{1-2y_{CO,in}-2y_{CO_2,in}}{(1-2y_{CO}-2y_{CO_2})^2}$$

For the direct synthesis process of alcohol/ether fuel, (23) can be written in the form

$$\frac{d(u_G C_{G,j})}{dl} \pm C_{cat} r_j = 0$$

(positive j=CO, CO_2, negative j=DME) (28)

Considering $C_{G,j} = \frac{N_j}{Au_G}$, substituting (22) into (28), and integrating, the differential equations of material balance for each key components in BCSR was given by

$$\begin{cases} \frac{dy_{CO}}{dl} = M \cdot T_f \left[\frac{(1-2y_{CO})r_{CO} - 2y_{CO}r_{CO_2}}{1-2y_{CO}-2y_{CO_2}}\right] \\ \frac{dy_{CO_2}}{dl} = M \cdot T_f \left[\frac{(1-2y_{CO_2})r_{CO_2} - 2y_{CO_2}r_{CO}}{1-2y_{CO}-2y_{CO_2}}\right] \\ \frac{dy_{DME}}{dl} = -M \cdot T_f \left[\frac{r_{DME} + 2y_{DME}(r_{CO}+r_{CO_2})}{1-2y_{CO}-2y_{CO_2}}\right] \end{cases} \quad (29)$$

where

$$M = -\frac{C_{cat}A}{N_{T,in} \cdot \frac{1-2y_{CO,in}-2y_{CO_2,in}}{(1-2y_{CO}-2y_{CO_2})^2}}$$

Substituting global kinetics equations and (24) into (29), the set of the differential equations (29) can be solved by the four-order Runge-Kutta-Felhberg numerical integration method using the following boundary condition.

at the inlet of the BCSR (l=0):

$$y_{CO} = y_{CO,in},\ y_{CO_2} = y_{CO_2,in},\ y_{DME} = y_{DME,in}$$

Combining with the material balance, numerical solutions of the molecule fraction of each component in the outlet of the BCSR are obtained. The determination of hydrodynamic and physical property correlations is listed in Table II.

For the coexistence of parallel hydrogenation of CO, CO_2 and water gas shift reaction, CO_2 was considered as either the reactants or products in different operation conditions and different syngas composition, the total carbon conversion and selectivity of DME/methanol were used for the purposes of quantitative determination of the effect of the operation conditions (temperature, pressure and weight hourly space velocity) on slurry catalyst. Given that the content of hydrocarbons as byproducts can be negligible, on the basis of feed and product flow rates and carbon balance, the total carbon conversion should be defined by

$$x_{TC} = 1 - \frac{N_{out}(y_{CO,out} + y_{CO_2,out})}{N_{in}(y_{CO,in} + y_{CO_2,in})} \quad (33)$$

and selectivity of DME/methanol is defined as follows

$$S_{DME} = \frac{2N_{out}y_{DME,out}}{N_{in}y_{CO,in} - N_{out}y_{CO,out}} \quad (34)$$

$$S_M = \frac{N_{out}y_{M,out}}{N_{in}y_{CO,in} - N_{out}y_{CO,out}} \quad (35)$$

TABLE II
HYDRODYNAMIC AND PHYSICAL PROPERTY CORRELATIONS

Relevant parameters	Correlations
Initial mass concentration of catalyst in the gas inlet	$C_{cat}^0 = \overline{C_{cat}} \cdot G / [\exp(G) - 1.0]$ where: $G = -\Psi_L u_p L_h / D_S$, $\Psi_L = 1 - \overline{C_{cat}}/\rho_p$, $u_p = 1.10 \cdot u_G^{0.026} u_t^{0.80} \Psi_L^{3.5}$
Grain sedimentation velocity u_t[16]:	$u_t = \frac{g d_p^2 (\rho_p - \rho_L)}{18\mu_L}$
Solid phase dispersion coefficient D_S[15]:	$\frac{u_G D_R}{D_S} = \left[9.6\left(Fr^6/\mathrm{Re}_g\right)^{0.1114} + 0.019\,\mathrm{Re}_p^{1.1}\right]$ where: $Fr = u_G/(gD_R)^{0.5}$, $\mathrm{Re}_p = u_t d_p \rho_L/\mu_L$, $\mathrm{Re}_g = u_G D_R \rho_L/\mu_L$
Gas holdup ε_G[17]:	$\varepsilon_G = 0.5863 u_G^{0.5159} W_{cat}^{-0.2454} \mu_L^{0.0073} \sigma^{0.1403}$
Density of liquid paraffin oil ρ_L[18]:	$\rho_L = 171.0 \times 0.1677^{-(1-T_r)^{2/7}}$ where: $T_r = T/916.18$
Viscosity of paraffin oil μ_L:	$\ln \mu_L = -3.0912 + 1.7038 \times 10^3 / T$
Surface tension of paraffin oil σ:	$\sigma_L = 50.7657 - 0.0737 \cdot T$

III. Results and Discussion

Using the simulation calculation program that we developed, the behavior of reactor design was carried out for DME direct synthesis from syngas in the bubble column slurry reactor of 10, 000t/a dimethyl ether under the typical industrial operating conditions that were as following: the feed composition of coal-based syngas: y_{H2} = 0.70, y_{N2} = 0.10, y_{CO} = 0.15, y_{CO2} = 0.05; reaction temperature: 240℃, reactor pressure: 5MPa, reactor diameter: 0.8m, catalyst content: 30%(wt), gas volumetric flux: 10000 $Nm^3 \cdot h^{-1}$. Meanwhile, it is also discussed in detail the influence of operation conditions and reactor diameter on reaction results with simulation results of the reactor design.

A. Axial Distribution of Catalyst Grain

1. Effect of Particles Diameter

Simulation results of catalyst axial concentration distribution were be carried out by varying the catalyst grain diameter in the range of 0.05-0.20mm, and maintaining the remaining

operating variables constant at the following values: reaction temperature, 513K; reactor pressure, 5MPa; reactor diameter, 0.8m; catalyst content, 30%(wt); superficial gas velocity, 0.1973m·s^{-1}. As be observed from Fig.1, the influence of catalyst particles diameter on the catalyst axial concentration distribution along the bed height is very important. The catalyst concentration distribution becomes well-distributed with the decreasing of particles diameter, and is almost uniform when the particles diameter is 0.05mm. This is due to the dual role of drag force of bubble phase on catalyst grains and sedimentation rate of catalyst grains in slurry phase which is increased with the increasing particles diameter, neglecting the influence of density of different catalysts.

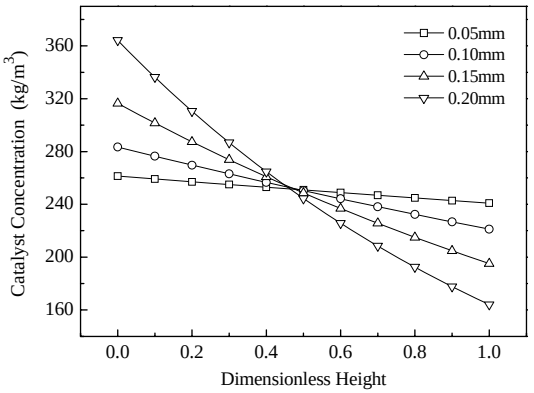

Fig. 1 Effect of particles diameter on catalyst axial concentration

2. Effect of Catalyst Content

The effect of catalyst content on the catalyst axial concentration distribution is shown in Fig.2. The result correspond to catalyst grain diameter of 0.060mm and the remaining operating conditions have been maintained constant at the following values: reaction temperature, 513K; reactor pressure, 5MPa; reactor diameter, 0.8m; superficial gas velocity, 0.1973m·s^{-1}. It has been observed that the tendency of the catalyst axial concentration distribution is almost uniform for the ultrafine catalysts grains of 0.060mm average diameter with the increasing of catalyst content in the range of 20%-35%(wt), the influence of catalyst content on the catalyst axial concentration distribution has been not obvious. Hence the DME direct synthesis process can be carried out under the slurry catalyst with a higher mass content to achieve higher methanol/DME yield.

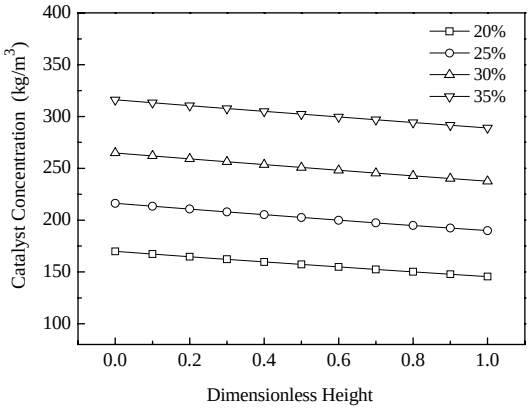

Fig. 2 Effect of catalyst content on catalyst axial concentration

3. Effect of Superficial Gas Velocity

The results of the catalyst axial concentration distribution were be carried out by varying superficial gas velocity in the range of 0.1142-0.2388 m/s, and the remaining operating conditions have been maintained constant at the following values: reaction temperature, 513K; reactor pressure, 5MPa; reactor diameter, 0.8 m; catalyst content, 30%(wt). As can be seen from Fig.3, the tendency of the catalyst axial concentration distribution is gradually close to uniform with the increasing of superficial gas velocity. It is a reasonable explanation that the drag force of bubble phase on catalyst grains increases with the increasing superficial gas velocity, and then sedimentation velocity of catalyst particles is slow down, which could lead to well distribution of catalyst axial concentration. It also can be obtained from Fig.3 that the varying of the superficial gas velocity has slightly influence on the catalyst axial concentration distribution.

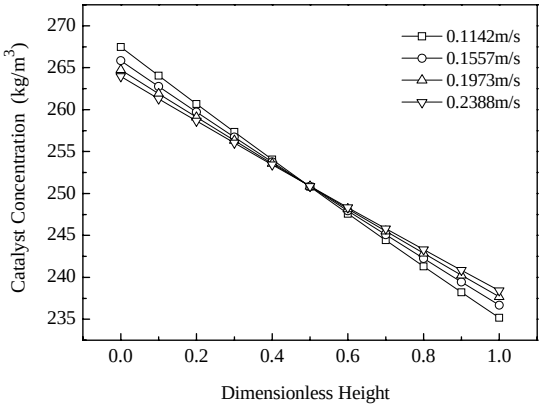

Fig. 3 Effect of superficial gas velocity on catalyst axial concentration

4. Effect of Reactor Diameter

The effect of reactor diameter on the catalyst axial concentration distribution along the bed height is shown in Fig.4. The result correspond to catalyst grain diameter of 0.060mm and the remaining operating conditions have been maintained constant at the following values: reaction temperature, 513K; reactor pressure, 5MPa; catalyst content,

30%(wt). From Figures 4, it is confirmed that the varying of the reactor diameter has heavily influence on the catalyst axial concentration distribution. In this case, superficial gas velocity and operating bed height are main factors influencing distribution uniformity. Kept gas normal volumetric flux in the inlet of BCSR constant, superficial gas velocity and operating bed height will be rapidly increased with the decreasing of reactor diameter because both of them are inversely proportional to quadratic power of reactor diameter. Meanwhile, because the effect of superficial gas velocity is slightly in coalesced bubble regime which has been previously discussed, a sharp increasing of operating bed height will be aggravated non-uniform distribution of catalyst axial concentration, especially in the slugging regime which is caused by high superficial gas velocity and minor reactor diameter.

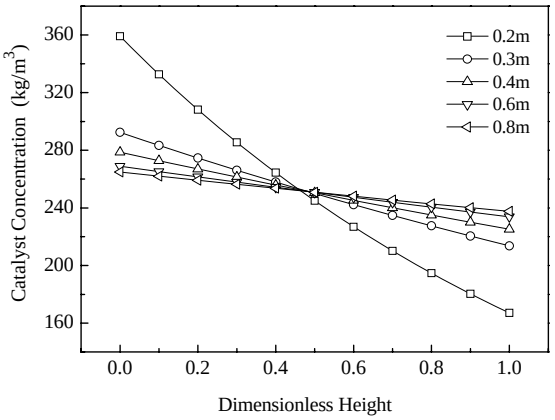

Fig.4 Effect of reactor diameter on catalyst axial concentration

5. Effect of Reactor Pressure

The effect of reactor pressure on the catalyst axial concentration distribution is shown in Fig.5. The result correspond to catalyst grain diameter of 0.060mm and the remaining operating conditions have been maintained constant at the following values: reaction temperature, 513K; reactor diameter, 0.8m; catalyst content, 30%(wt). It can be obtained that the decreasing of the reactor pressure has slightly effect on the catalyst axial concentration distribution uniformity. Gas normal volumetric flux remaining unchanged, superficial gas velocity will be increased with the decreasing of reactor pressure, and then improve axial uniform distribution of catalyst particles. By comparing and analyzing factor trend in the Fig.3 and Fig.5, it is clear that a similar trend by the decreasing of reactor pressure or the increasing of superficial gas velocity.

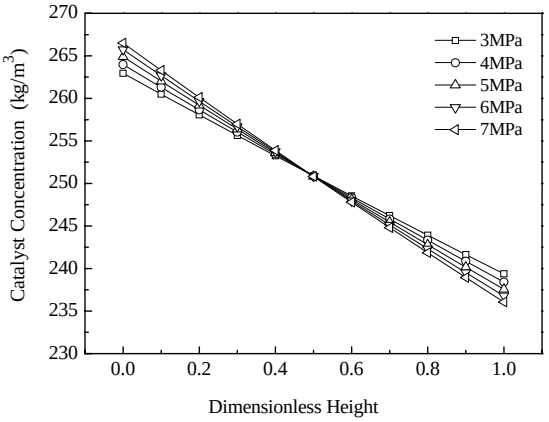

Fig.5 Effect of reactor pressure on catalyst axial concentration

6. Effect of Reaction Temperature

The effect of reaction temperature on the catalyst axial concentration distribution is shown in Fig.6. The result correspond to catalyst grain diameter of 0.060mm and the remaining operating conditions have been maintained constant at the following values: reactor pressure, 5MPa; reactor diameter, 0.8m; catalyst content, 30%(wt). The influence of reaction temperature should be discussed from the following two aspects: one is that physical properties of liquid paraffin (viscosity and density) are function of reaction temperature, and both of them are reduced with the increasing of the reaction temperature, which can lead to the nonuniformity of catalyst particles axial concentration distribution; another is that superficial gas velocity in bubble column bed is increased with the increasing of the reaction temperature, which can improve the uniformity of catalyst particles axial concentration distribution. By taking the two aspects into consideration, the reaction temperature has little or no influence on the catalyst axial concentration distribution.

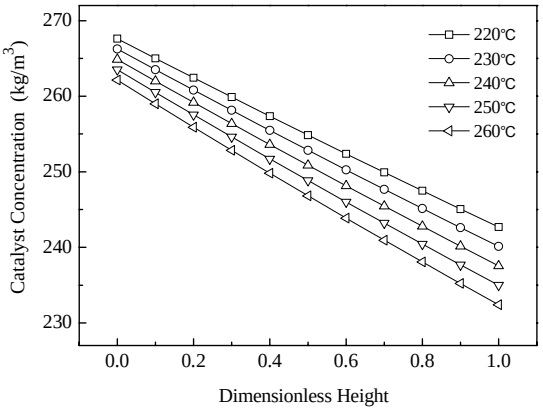

Fig. 6 Effect of reaction temperature on catalyst axial concentration

B. Discussion of Model Simulation Results

1. Effect of Reaction Temperature

The influence of reaction temperature on static bed height and slurry operating bed height with model simulation results in BCSR is shown in Fig.7, and the effect of reaction

temperature on total carbon conversion and selectivity of DME and on production capacity of products with model simulation results in BCSR are shown in Fig.8- Fig.9, respectively. As can be seen, the total carbon conversion, selectivity and yield of DME decrease slightly with increasing temperature in the range of 220-260℃, which is in accordance with thermodynamic characteristic that higher temperatures is unfavorable to equilibrium conversion of syngas since DME direct synthesis reaction is an exothermic reaction. And it is found that each reaction is close nearly to the state of chemical equilibrium by comparison between experimental and simulation values of equilibrium constants of each reaction in the outlet of the reactor. It can be obtained from Fig.7 that the static bed height and operating bed height drop suddenly as the temperature increases, even though the average gas holdup and superficial space velocity don't change obviously. This is the result that the reaction rate of each product is improved with increasing temperature. By taking into consideration the combination of economic benefits of dimethyl ether and equipment investment of bed height, it is advised that the optimal reaction temperature should be about 240℃ in the DME synthesis process.

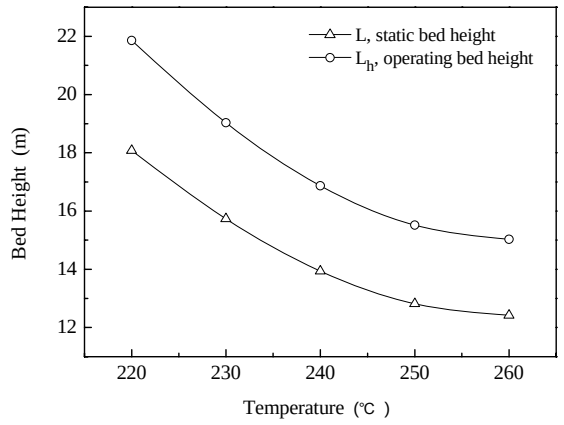

Fig.7 Effect of reaction temperature on bed height

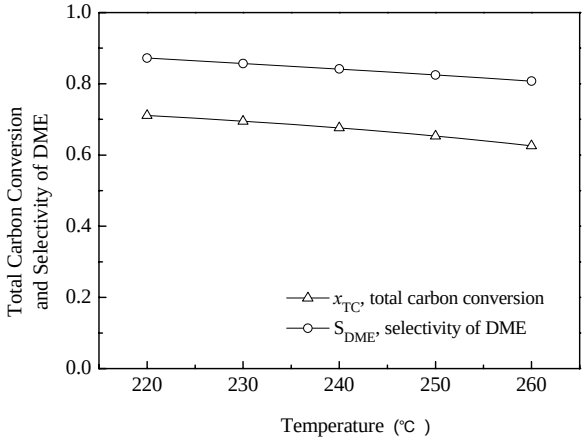

Fig. 8 Effect of reaction temperature on total carbon conversion and selectivity of DME

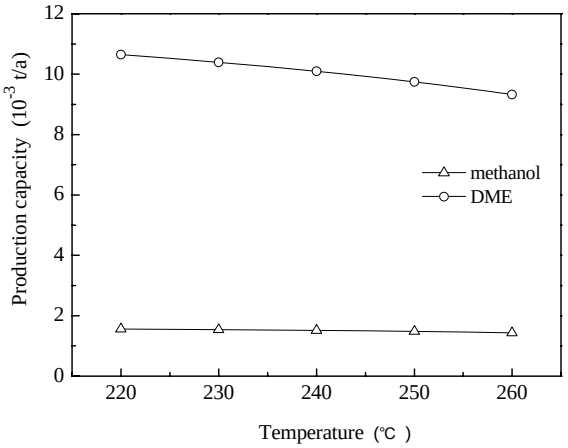

Fig. 9 Effect of reaction temperature on production capacity

2. Effect of Reactor Pressure

The influence of reactor pressure on the static bed height and the slurry operating bed height with model simulation results in BCSR is shown in Fig.10, and the effect of reactor pressure on total carbon conversion and selectivity of DME and on production capacity of products with model simulation results in BCSR are shown in Figures 11 and 12, respectively. It is confirmed that total carbon conversion, selectivity of DME and yield of methanol/DME are all increased as reactor pressure increases in the range of 3-7Mpa, which is based on the fundamentals that increasing pressure is favorable to DME direct synthesis process for stoichiometric-number-reducing reaction. It is obvious that when the reactor pressure is increased, average gas holdup and superficial space velocity are declined obviously. As a result, the operating bed height is decreased greatly, while the static bed height decreases slightly. It seems that higher pressure is favorable to DME direct synthesis process with all simulation results, but considering that the slurry reactor is also a pressure vessel, it is rather high of equipment investment, operation cost and energy consumption in this case. It is proposed that 5MPa is the optimal reactor pressure of DME synthesis process for commercial scale.

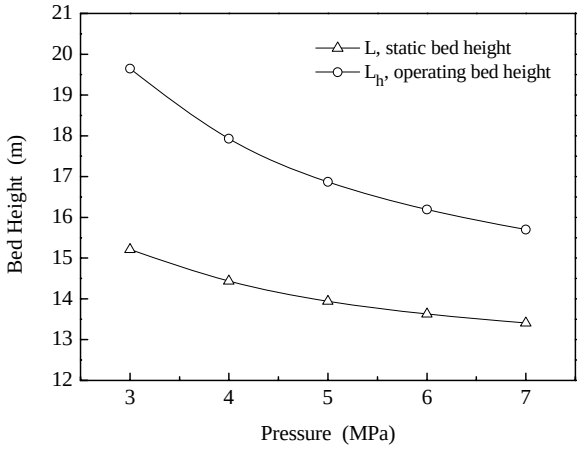

Fig. 10 Effect of reactor pressure on bed height

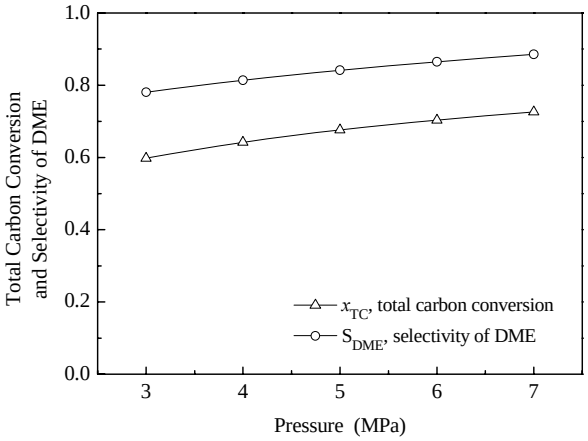

Fig.11 Effect of reactor pressure on total carbon conversion and selectivity of DME

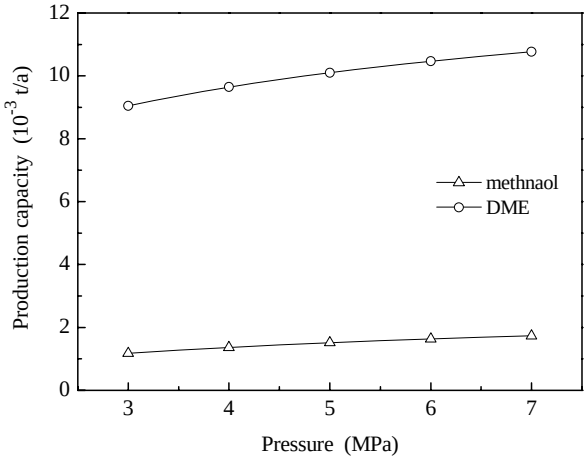

Fig. 12 Effect of reactor pressure on production capacity

3. Effect of Reactor Diameter

The influence of the reactor diameter on the static bed height and the slurry operating bed height with model simulation results in the BCSR is shown in Fig.13, and the effect of the reactor diameter on total carbon conversion and selectivity of DME and on production capacity of products with model simulation results in BCSR are shown in Fig.14-Fig.15 respectively. As is observed, total carbon conversion, selectivity of DME, and yield of methanol/DME are kept almost constant with a reactor diameter in the range of 0.6-1.0 m. But both the operating bed height and the static bed height are increased obviously because the average gas holdup and superficial space velocity are increased as the reactor diameter decreases. Considering the double influences of the diameter and the height of the reactor on unit investment, the reactor diameter of 0.8m was suggested to aim at a suitable ratio of height to diameter for the reactor design of DME direct synthesis process.

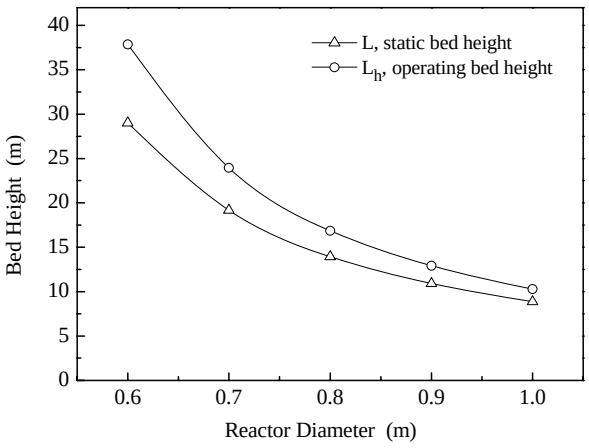

Fig. 13 Effect of reactor diameter on bed height

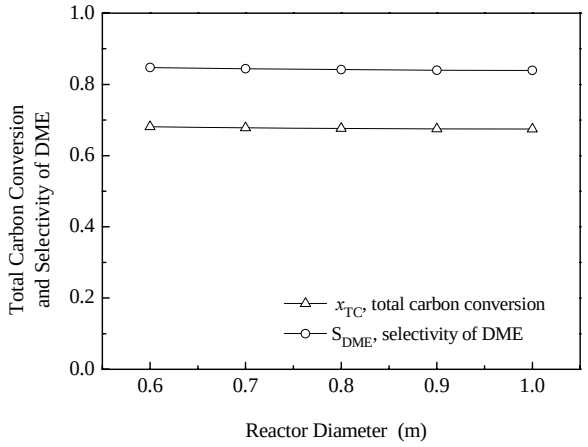

Fig. 14 Effect of reactor diameter on total carbon conversion and selectivity of DME

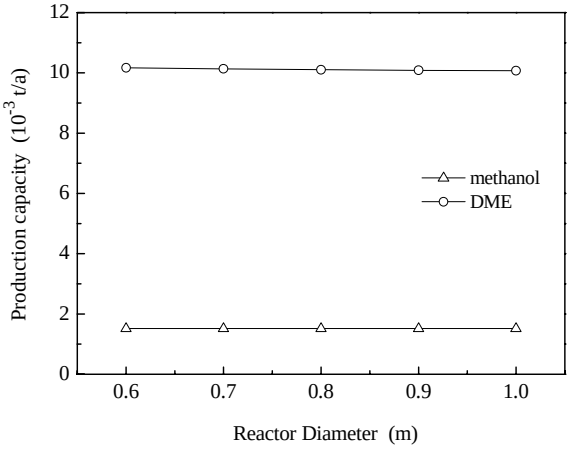

Fig. 15 Effect of reactor diameter on production capacity

IV. Conclusion

A steady-state one-dimensional mathematical model for three-phase bubble column slurry reactor has been established based on the assumptions of plug flow of gas phase, catalyst

grains sedimentation-dispersion model and isothermal process in the whole reactor bed. It is discussed in detail the influence of operation conditions on catalyst axial concentration distribution with simulation results based on sedimentation-dispersion model, from which it can be obtained that the particle diameter and reactor diameter are the main two factor influencing concentration distribution uniformity.

The influence of the construction parameters of the reactor and operation parameters of DME synthesis industrial demonstration unit was also determined. It can be obtained that higher pressure and lower temperature were beneficial to the increase of CO conversion, DME selectivity and products yield, and that height of slurry bed is lessen with the increasing of operation temperature in the range of 220-260℃. The optimal operation conditions in BCSR were proposed: temperature at 240℃, pressure at 5MPa and reactor diameter of 0.8m.

NOMENCLATURE

A: reactor bed cross-sectional area, m^2
a_L: specific surface area of gas-liquid mass transfer, $m^2 \cdot m^{-3}$
a_S: specific surface area of particles, $m^2 \cdot m^{-3}$
C_{cat}: catalyst mass concentration in slurry phase, $kg \cdot m^{-3}$
$\overline{C_{cat}}$: average mass concentration of catalyst in reactor, $kg \cdot m^{-3}$
C_{cat}^0: initial mass concentration of catalyst in the gas inlet, $kg \cdot m^{-3}$
$C_{G,j}$: concentration of gas phase component j, $kmol \cdot m^{-3}$
$C_{G,j}^*$: equilibrium concentration of gas phase component j at gas-liquid interface, $kmol \cdot m^{-3}$
$C_{L,j}$: concentration of liquid phase component j, $mol \cdot m^{-3}$
$C_{S,j}$: concentration of liquid phase component j on the surface of catalyst, $kmol \cdot m^{-3}$
D_R: internal diameter of BCSR, m
D_G: axial back-mixing diffusion coefficient in gas phase, $m^2 \cdot s^{-1}$
D_L: axial back-mixing diffusion coefficient in slurry phase, $m^2 \cdot s^{-1}$
D_S: axial dispersion coefficient of catalyst particles, $m^2 \cdot s^{-1}$
d_p: average diameter of catalyst particles, m
f_j: fugacity of component j, Pa
G: gravitational acceleration, $m \cdot s^{-2}$
$k_{L,j}$: liquid mass transfer coefficient of component j at gas-liquid interphase, $m \cdot s^{-1}$
$k_{S,j}$: liquid mass transfer coefficient of component j at liquid-solid interphase, $m \cdot s^{-1}$
L: static bed height, m
L_h: slurry operating bed height, m
m: gas-liquid equilibrium constant
N_j: transient flux of component j in reactor bed, $mol \cdot s^{-1}$
N_T: transient flux of gas in reactor bed, $mol \cdot s^{-1}$
$N_{T,in}$: inlet flux of syngas, $mol \cdot s^{-1}$
$r_{i,j}$: reaction rate of component j involved in chemical reaction i, $kmol \cdot kg^{-1} \cdot s^{-1}$
r_j: reaction rate of component j, $kg \cdot m^{-1} \cdot s^{-1}$
R: gas constant, $kJ \cdot kmol^{-1} \cdot K^{-1}$
S_{DME}: selectivity of dimethyl ether
T: reaction temperature, K
u_G: superficial gas velocity, $m \cdot s^{-1}$
V_{cat}: volume fraction of catalyst in slurry phase without syngas in
W: weight of catalyst, kg
W_{cat}: mass fraction of catalyst particles in slurry phase, w.%
y_j: mole fraction of component j in gas phase
β_{WGS}: equilibrium degree of water-gas shift reaction
ε_G: gas holdup
$v_{i,j}$: stiochoimetric coefficient of component j involved in chemical reaction i
ρ_p: density of catalyst particles, $kg \cdot m^{-3}$

Superscripts:
*: indicate equilibrium value
0: indicate initial value

Subscripts
cal: calculated value
cat: catalyst
exp: experimental value
G: gas phase
in: at the inlet of reactor bed
L: liquid phase
out: at the outlet of reactor bed
P: catalyst particles
S: solid phase
T: total
WGS: water-gas shift reaction

REFERENCES

[1] K. D. P. Nigam, A. Schumpe, Three-phase Sparged Reactors. London: Gordon and Breach Science Publishers, 1996, ch. 5-6, pp. 339-422.
[2] A. T. Aguayo, J. Ereña, I. Sierra, M. Olazar, J. Bilbao, "Deactivation and regeneration of hybrid catalysts in the single-step synthesis of dimethyl ether from syngas and CO_2," Catalysis Today, vol. 106, no. 1-4, pp. 265–270, Oct. 2005.
[3] J. Ereña, R. Garoña, J. M. Arandes, A.T. Aguayo, J. Bilbao, "Effect of operating conditions on the synthesis of dimethyl ether over CuO-ZnO-Al_2O_3/NaHZSM-5 bifunctional catalyst," Catal. Today, vol. 107-108, pp. 467-473, Oct. 2005.
[4] A.T. Aguayo, J. Ereña, D. Mier, J. M.Arandes, M. Olazar, J. Bilbao, "Kinetic modeling of dimethyl ether synthesis in a single step on a CuO-ZnO-Al_2O_3/γ-Al_2O_3 catalyst," Ind. Eng. Chem. Res., vol. 46, no. 17, pp. 5522-5530, July. 2007.
[5] Z.-H. Gao, W. Huang, J.-Y. Wang, L.-H. Yin, K.-C. Xie, "Complete liquid-phase preparation and characterization of Cu-Zn-Al-Zr slurry catalysts for synthesis of dimethyl ether," Acta Chimica Sinica, vol. 66, no. 3, pp. 295-300, Feb. 2008.
[6] D. Song, W. Cho, G. Lee, D. K. Park, E. S. Yoon, "Numerical analysis of a pilot-scale fixed-bed reactor for dimethyl ether (DME) synthesis," Ind. Eng. Chem. Res., vol. 47, no. 13, pp. 4553-4559 May. 2008.
[7] W.-Z. Lu, L.-H. Teng, W.-D. Xiao, "Simulation and experiment study of dimethyl ether synthesis from syngas in a fluidized-bed reactor," Chem. Eng. Sci., vol. 59, no.22-23, pp.5455-5464, Nov-Dec. 2004.
[8] Z.-G. Nie, H.-W. Liu, D.-H. Liu, W.-Y. Ying, D.-Y. Fang, "The global kinetics of synthesis of dimethyl ether from syngas containing N_2 over bifunctional catalyst," Chemical Reaction Engineering and Technology, vol. 20, no. 1, pp. 1-7, Mar. 2004.
[9] D.-H. Liu, X. Hua, D.-Y. Fang, "Mathematical Simulation and Design of three-phase bubble column reactor for direct synthesis of dimethyl ether from syngas," Journal of Natural Gas Chemistry, vol. 16, no.2, pp. 193-199, Apr. 2007.
[10] W.-D. Song, B.-C. Zhu, Z.-C. Luo, L.-B. Yu, G.-X. Feng, X. Xu, "Computation for heat of reaction and equilibrium constant of methanol synthesis under pressure by using SHBWR equation of state," Journal of East China University of Science and Technology, vol. 17, no. 1, pp. 11-24, Jan. 1981.
[11] Q. Zhang, J. Yang, W.-Y. Ying, D.-Y.Fang, "Calculation of equilibrium conversion and selectivity for dimethyl ether synthesis from syngas," Chemical Engineering, vol. 33, no. 2, pp. 64-68, Apr. 2005.
[12] Y.-L. Zhao, "Mathematical model for bubble column slurry reactor," Chemical Engineering, vol. 19, no. 5, pp. 13-21, Oct. 1991.
[13] V. M. H. Govindarao, "On the dynamics of bubble column slurry reactors," Chem. Eng. J., vol. 9, no. 3, pp. 229-240, June. 1975.
[14] V. M. H. Govindarao, M. Chidambaram, "Semibatch bubble-column slurry reactors: effect of dispersion on the steady-state behavior," AIChE J., vol. 30, no. 5, pp. 842-845, Sept .1984.
[15] D. N. Smith, J. A. Ruether, "Dispersed solid dynamics in a slurry bubble column," Chem. Eng. Sci., vol. 40, no. 5, pp. 741-754, May. 1985.
[16] M.-H. Chen, Principles of Chemical Industry (volume two). Beijing: Chemical Industry Press, 2000, ch. 5, pp. 197.
[17] B.-Q. Ding, J.-B. Zhang, D.-Y. Fang, B.-C. Zhu, "Hydrodynamic study of three-phase slurry reactor with high solid concentration," Journal of East

China University of Science and Technology, vol. 26, no. 3, pp. 22-231, June. 2000.
[18] H.-F. Qin, S.-R. Wang, B.-Q. Ding, B.-C. Zhu, "Determination and estimation of physical property data for liquid paraffin," Natural Gas Chemical Industry, vol. 24, no. 3, pp. 56-58, June. 1999.